Diffraction-induced transformation of near-cycle and subcycle pulses

A. E. Kaplan

Department of Electrical and Computer Engineering, The Johns Hopkins University, Baltimore, Maryland 21218

Received July 28, 1997; revised abstract received October 29, 1997

An analytical approach to the theory of diffraction transformation of pulses with superbroad spectra and arbitrary time dependence, in particular half-cycle (unipolar), single-cycle, and multicycle pulses, was developed. Closed-form solutions were found for on-axis propagation of half-cycle pulses with initially Gaussian spatial profiles that have either $\cosh^{-1}$-like or Gaussian time dependence, for single-cycle pulses based on higher modes of these functions, and for multicycle pulses. The far-field propagation demonstrates common patterns of time-derivative behavior regardless of the initial spatiotemporal profile. It is also shown that the time width of an off-axis pulse increases with the angle of observation. Owing to time–space reciprocity, the pulse transformation that is due to diffraction can be reversed, e.g., by reflection of a pulse from a spherical concave mirror. © 1998 Optical Society of America [S0740-3224(98)03603-0]

OCIS codes: 320.2250, 050.1960, 260.1960, 320.5540, 170.6920, 320.5550.

1. INTRODUCTION

Diffraction is one of the fundamental manifestations of the wave nature of light. The diffraction theory of monochromatic light has been developed in great detail (see, e.g., Ref. 1). In general this theory is heavily mathematically loaded, but the development of lasers advanced the use of Gaussian beams, which are automodel solutions of a so-called paraxial approximation (PA) and allow one to handle the diffraction of spatially smooth optical beams in a simple way (see, e.g., Ref. 2). Recent developments[3–7] in optics resulted in the generation of short and intense EM pulses of a nonoscillatory nature, or almost unipolar half-cycle pulses (HCP's), with extremely broad spectra that start at zero frequency. Their applications range from the time-domain spectroscopy[3] of dielectrics, semiconductors, and flames[4] and of transient chemical processes such as dissociation and autoionization,[5] to new principles of imaging[6] and to atomic physics by means of photoionization.[7] The spectra of currently available HCP's generated in semiconductors by means of optical rectification reach into the terahertz domain; they are approximately 400–500 fs wide, with the peak field up to 150–200 kV/cm. Recently the author and co-workers[8,9] proposed two new different principles of generating much shorter (down to 0.1 fs = 10^{-16} s) and stronger (up to $\sim 10^{16}$ W/cm^2) HCP's. One of these principles is based on stimulated cascade Raman scattering[8] and would result in the generation of an almost periodic train of powerful subfemtosecond pulses, and another one, based on the generation of EM bubbles,[9] would generate unipolar EM solitons propagating in a gas of two-level or classically nonlinear atoms.

Inasmuch as different frequency components in HCP's diffract differently, far away from the source HCP's propagate with significant dispersion and distortion, even in free space.[3–7,10,11] This phenomenon calls for the diffraction–transformation theory of pulses with superbroad spectra, preferably comparable in its simplicity and insights with that of Gaussian beam diffraction of monochromatic light. Such a theory could also apply to other fields of wave physics: acoustics, solid-state physics, and quantum mechanics.

It is well known by now[3–7,10] that near-cycle and subcycle pulses, as they propagate, undergo a transformation resembling the action of a high-pass filter; in particular, in the far-field area they show time-derivative behavior. This behavior was verified in numerical simulation[11] of the propagation of a half-cycle pulse with an (initially) Gaussian spatial profile. In Ref. 11 only the fields with an also (initially) Gaussian temporal profile were considered. However, even for that profile, no analytical solution (at least for on-axis propagation of a pulse) for the field behavior along the entire propagation path was found, leaving the theory without the major advantage of a standard theory of monochromatic Gaussian beams. The ability of theory to address the propagation between near- and far-field areas is essential, because in practice that intermediate area could be of most significance, with the diffraction distance for the highest spectral frequency,

$$z_d = r_0^2/ct_0, \tag{1.1}$$

(where $2t_0$ is a pulse time–width and $2r_0$ is a pulse's transverse size) being considerably large. For $2t_0 \sim 400$ fs and $2r_0 \sim 1$ cm,[3–7] one has $z_d \sim 40$ cm, the same as, e.g., for $2t_0 \sim 4$ fs and $2r_0 \sim 1$ mm.

In this paper we derive a simple equation for an on-axis field (with a Gaussian initial spatial profile) that is valid for an arbitrary temporary profile and for any distance from the source. Using that equation, we obtain closed-form solutions for the field transformation that is due to diffraction for some standard temporal profiles and show that in the far-field area pulses demonstrate time-derivative behavior regardless of their initial time depen-

dence. Furthermore, in the low- (compared with the inverse source size) frequency limit we find a general solution valid for any spatial and temporal profiles of the field, which also explains in simple antenna terms the nature of time-derivative behavior; this solution is also valid in the far-field area for any frequency. We also demonstrate that the pulse transformation that is due to diffraction can be reversed, e.g., by reflection of a pulse from a spherical concave mirror; this effect is based on the time–space reciprocity of pulse propagation.

2. EQUATION OF ON-AXIS PROPAGATION AND ITS GENERAL PROPERTIES

Consider a pulse propagating along the z axis and having an arbitrary time dependence and a known transverse profile at the source, $z = 0$. At this point we assume a high-frequency limit, meaning that the shortest temporal scale of the pulse, t_0 (in the extreme case of a nonoscillating, half-cycle pulse it is its initial half-time width; see below), and its respective longitudinal scale, ct_0, are much shorter than its transverse radius, r_0:

$$r_0 \gg ct_0 \quad \text{or} \quad z_d/r_0 \gg 1. \tag{2.1}$$

The frequency components of the largest part of its spectrum, $c/r_0 < \omega < {t_0}^{-1}$, will propagate with relatively small diffraction, so one can apply a standard paraxial approximation PA to each one of them. Within the PA the diffraction of a monochromatic field, $E_\omega \exp[-i\omega(t - z/c)]$, in free space is described by use of a PA wave equation similar to a Schrödinger equation for a free electron:

$$-2i(\omega/c)\partial E_\omega/\partial z + \Delta_\perp E_\omega = 0, \tag{2.2}$$

where $\Delta_\perp$ is a transverse Laplacian; note that the PA allows one to neglect polarization of the field and reduce the problem to a scalar one. We also assume that the field is cylindrically symmetric in its cross section, so $\Delta_\perp = \partial^2/\partial r^2 + r^{-1}\partial/\partial r$, where r is the radial distance from the z axis in the cross section. Equation (2.2) for the field E_ω behavior in the Fourier domain can also be translated into the time-domain PA equation for $E_{\tilde{t}}$ as

$$-2(\partial^2 E_{\tilde{t}}/\partial z\,\partial\tilde{t}) + c\Delta_\perp E_{\tilde{t}} = 0, \tag{2.3}$$

where $\tilde{t} = t - z/c$ is a retarded time. Our approach to studying time-domain behavior of E_t in this paper is based on using Fourier-domain equation (2.2) to find the transformation of the original spectrum of the field and translating the transformed spectrum back into the time domain. With most of the available or to-be-available sources of HCP's one can assume that the field at the source has a plane phase front for all the spectral components, so their waists are located at the source. The spatially Gaussian field at the source, $z = 0$, can then be written as

$$E_{z=0} = E_0(t)\exp(-r^2/2{r_0}^2), \tag{2.4}$$

where r_0 is the radius of the spatial field profile at the level $\exp(-1/2)$ of peak amplitude, $\mathscr{E}_0$. Writing the solution of PA equation (2.2) as a Fourier transform:

$$E(\tilde{t}, r, z) = (2\pi)^{-1/2}\int_{-\infty}^{\infty} S(\omega, r, z)\exp(i\omega\tilde{t})\mathrm{d}\omega, \tag{2.5}$$

we have the field spectrum $S(\omega, r, z)$ for a Gaussian mode as

$$S(\omega, r, z) = D(\omega, z)S_0(\omega)\exp[-(r^2/2{r_0}^2)D(\omega, z)], \tag{2.6}$$

where $S_0(\omega) = (2\pi)^{-1/2}\int_{-\infty}^{\infty} E_0(t)\exp(-i\omega t)\mathrm{d}t$ is the spectrum of original pulse and

$$D(\omega, z) = (1 - izc/\omega{r_0}^2)^{-1} \tag{2.7}$$

is a diffraction factor that is due to the PA. For the on-axis field, $r = 0$, we have

$$S_{\mathrm{on}}(\omega, z) = D(\omega, z)S_0(\omega) = i\nu(\zeta + i\nu)^{-1}S_0(\nu), \tag{2.8}$$

where $\nu \equiv \omega t_0$. By substituting Eq. (2.8) into Eq. (2.5) and introducing also a dimensionless retardation time $\tau \equiv (t - z/c)/t_0$ and a propagation distance $\zeta \equiv z/z_d = zct_0/{r_0}^2$, we derive a simple equation for the temporal dynamics of an on-axis field at any point ζ:

$$\partial E_{\mathrm{on}}/\partial\tau + \zeta E_{\mathrm{on}} = \partial E_0(\tau)/\partial\tau. \tag{2.9}$$

If the full energy of the field at source is finite, the solution for the on-axis field is

$$E_{\mathrm{on}}(\tau, \zeta) = E_0(\tau) - \zeta\exp(-\zeta\tau)\int_{-s(\zeta)\infty}^{\tau}\exp(\zeta t)E_0(t)\mathrm{d}t, \tag{2.10}$$

where $s(x) = -1$ if $x < 0$ and $s(x) = 1$ otherwise. One can see that, as expected, in a near-field area, $\zeta \ll 1$, the original temporal pulse profile is almost conserved, $E_{\mathrm{on}}(\tau) \sim E_0(\tau)$. The most interesting and universal (see below) pulse transformation occurs in far-field area, $\zeta \gg 1$. In this case E_{on} can be expanded as

$$E_{\mathrm{on}}(\tau, \zeta) = -\sum_{n=1}^{n=\infty}\frac{1}{(-\zeta)^n}\frac{\partial^n E_0(\tau)}{\partial\tau^n}, \tag{2.11}$$

so, as $\zeta \to \infty$, the on-axis far field replicates the time derivative of the original pulse:

$$E_{\mathrm{on}}(\tau, \zeta) \to \zeta^{-1}\partial E_0(\tau)/\partial\tau. \tag{2.12}$$

All the results [Eqs. (2.8)–(2.12)] are true for an arbitrary initial temporal profile, $E_0(\tau)$. In particular, any HCP is transformed in the far-field area into a single-cycle pulse.

Writing Eq. (2.9) in real time, $\partial E_{\mathrm{on}}/\partial\tilde{t} + E_{\mathrm{on}}/T = \partial E_0/\partial\tilde{t}$, where $T = t_0\zeta^{-1} = {r_0}^2/cz$, we notice that it coincides with an equation for the voltage $U_R \propto E_{\mathrm{on}}$ at a resistor R in a series RC circuit (high-pass filter) driven by a source $U_S \propto E_0(\tilde{t})$, so the circuit relaxation time is $T = RC$. Because the only parameter with the dimensionality of resistance in a free-space propagation is the wave impedance of vacuum ($R = 120\pi\ \Omega$), the circuit capacitance is then $C \propto {r_0}^2/z$, which is consistent with a capacitor formed by electrodes having the pulse waist area $\propto {r_0}^2$ and spaced by z and thus provides an interesting and simple interpretation of the nature of pulse transformation in free space.

3. HALF-CYCLE PULSES: ANALYTICAL SOLUTIONS FOR ON-AXIS PROPAGATION

Although Eqs. (2.9) and (2.10) provide a general solution for the on-axis field evolution along the entire path of propagation (i.e., for an arbitrary ζ), it is important to have meaningful examples of an initial field profile whereby the integrals in Eq. (2.10) are solved analytically in closed form. In this section we consider two such examples for half-cycle pulses; in Section 4 we consider also two examples of single-cycle pulses.

One such example of the former kind of pulse is given by a smooth bell-shaped initial profile:

$$E_0(\tau) = \mathscr{E}_0(1 + |\tau|)\exp(-|\tau|) \tag{3.1}$$

with almost exponential wings at $|\tau| \to \infty$. Equation (2.10) then yields

$$\frac{E_{\text{on}}(\tau, \zeta)}{\mathscr{E}_0} = \frac{\exp(-|\tau|)}{1 - s(\tau)\zeta}\left[\frac{1}{1 - s(\tau)\zeta} + |\tau|\right] + \frac{2\zeta \exp(-\zeta\tau)[s(\zeta) + s(\tau)]}{(1 - \zeta^2)^2}. \tag{3.2}$$

At the point $\zeta = 1$ and $\tau > 0$, where the denominators in Eq. (3.2) zero out, one can show that the right-hand side of Eq. (3.2) is $\exp(-\tau)(1 - 2\tau^2)/4$.

It is interesting to note that for a familiar profile

$$E_0 = \mathscr{E}_0/\cosh(\tau), \tag{3.3}$$

a closed-form analytical solution [Eq. (2.10)] in elementary functions exists only if ζ is any rational number, but the form of this solution is different for different values of ζ. For example, at $\zeta = 1$, one has $E_{\text{on}}(\tau, 1) = E_0(\tau) - \mathscr{E}_0 \exp(-\tau)\ln[1 + \exp(2\tau)]$.

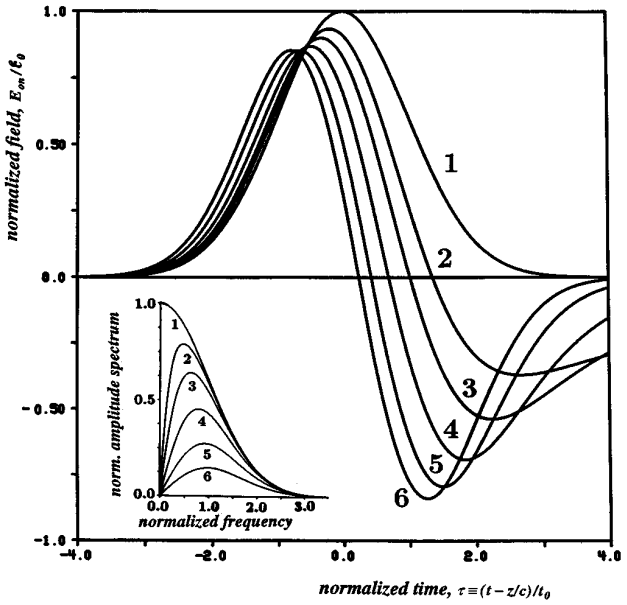

Fig. 1. Evolution of the on-axis temporal profile. The curves depict the normalized field $\mathbf{E}_{\text{on}}/\mathscr{E}_0$ versus the normalized time $\tau = t/t_0$ and the normalized amplitude spectrum $|S|/\mathscr{E}_0 t_0$ versus the normalized frequency $\nu \equiv \omega t_0$ (inset) of the initially Gaussian half-cycle pulse [Eq. (3.4)] as it propagates along the axis $\zeta = zct_0/r_0^2$. Curves: 1, $\zeta = 0$; 2, $\zeta = 0.25$; 3, $\zeta = 0.5$; 4, $\zeta = 1$; 5, $\zeta = 2$; 6, $\zeta = 4$. For comparison, each curve in the larger part of the figure is scaled up by the factor $w^{-1/2}(\zeta)$.

Another example of the initial temporal profile amenable to a closed-form analytic solution is a Gaussian profile:

$$E_0(t) = \mathscr{E}_0 \exp(-t^2/2t_0^2) = \mathscr{E}_0 \exp(-\tau^2/2) \tag{3.4}$$

[here t_0 is the pulse half-width at $\exp(-1/2)$ amplitude peak], which has the spectrum $S_0 = \mathscr{E}_0 t_0 \exp(-\omega^2 t_0^2/2)$ and is handled analytically for any ζ:

$$E_{\text{on}}(\tau, \zeta) = E_0(\tau)(1 - \zeta(\pi/2)^{1/2} \exp[(\tau - \zeta)^2/2] \times \{s(\zeta) + \text{erf}[(\tau - \zeta)/\sqrt{2}]\}), \tag{3.5}$$

where $\text{erf}(x) \equiv 2\pi^{-1/2}\int_0^x \exp(-x^2)\text{d}x$.[12] Note that for both of these signals [Eqs. (3.1) and (3.4)] the solution is centrosymmetric, $E_{\text{on}}(\tau, \zeta) = E_{\text{on}}(-\tau, -\zeta)$. As the pulse propagates, its total on-axis energy per unity area,

$$W_{\text{on}}(\zeta) = \int_{-\infty}^{\infty} |S_{\text{on}}(\omega, \zeta)|^2 \text{d}\omega = \int_{-\infty}^{\infty} E^2(t, \zeta)\text{d}t, \tag{3.6}$$

decreases as

$$w(\zeta) \equiv W_{\text{on}}(\zeta)/W_{\text{on}}(0) = 1 - \zeta\sqrt{\pi} \exp(\zeta^2)[s(\zeta) - \text{erf}(\zeta)], \tag{3.7}$$

which in the limit $\zeta \to \infty$ yields $w(\zeta) \to (2\zeta^2)^{-1}$, as expected. The evolution of the profile and the spectrum of the on-axis Gaussian HCP as it propagates away from the source is shown in Fig. 1; one can clearly see that the pulse sheds lower frequencies to form finally an almost-exact mimic of the time derivative of the original Gaussian pulse. The zero point (i.e., the moment τ_z at which $E = 0$), is moving closer to $\tau = 0$ as the distance $\zeta \gg 1$ increases. Using first two terms in Eq. (2.11), with the zero point found from $\tau_z \partial E/\partial\tau \approx \partial^2 E/\partial\tau^2$, we have $\tau_z \approx \zeta^{-1}$.

4. SINGLE-CYCLE PULSES: ANALYTICAL SOLUTIONS FOR ON-AXIS PROPAGATION

The higher-order modes of the half-cycle profiles [Eqs. (3.1) and (3.4)] can readily be used to yield closed-form analytical solutions for single-cycle, 3/2-cycle, two-cycle, etc. pulses. We consider here two examples of single-cycle pulses amenable to closed-form solutions.

First, similarly as for Eq. (3.1), consider a single-cycle pulse with almost exponential wings:

$$E_0(\tau) = \mathscr{E}_0\tau(1 + |\tau|)\exp(-|\tau|) \tag{4.1a}$$

or, even more simply,

$$E_0(\tau) = \mathscr{E}_0\tau \exp(-|\tau|). \tag{4.1b}$$

Equation (2.10) then yields, when it is applied to Eq. (4.1b),

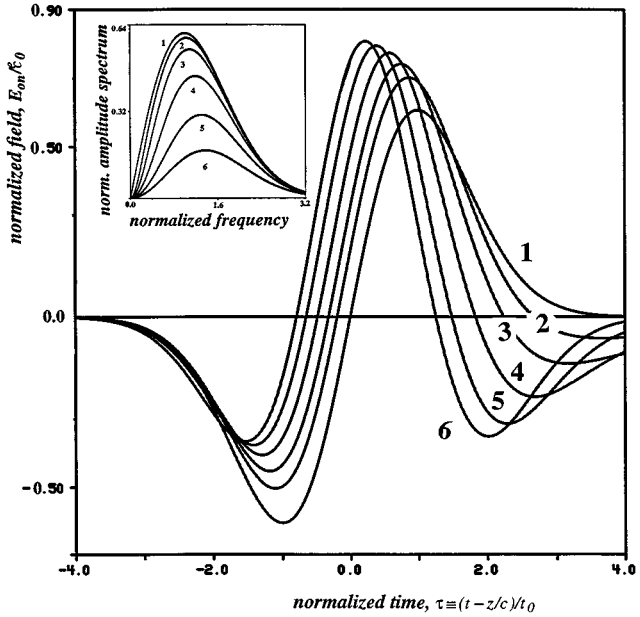

Fig. 2. Same as Fig. 1, but for the initially Gaussian single-cycle pulse [Eq. (4.3)].

$$\frac{E_{on}(\tau,\zeta)}{\mathscr{E}_0} = \frac{\exp(-|\tau|)}{1 - s(\tau)\zeta}\left[\frac{\zeta}{1 - s(\tau)\zeta} + \tau\right] - \frac{2\zeta^2 \exp(-\zeta\tau)[s(\zeta) + s(\tau)]}{(1 - \zeta^2)^2}. \quad (4.2)$$

The other example is a first higher mode of a Gaussian pulse [Eq. (3.4)]:

$$E_0(t) = \mathscr{E}_0 \tau \exp(-\tau^2/2), \qquad \tau = t/t_0, \quad (4.3)$$

which has the spectrum $S_0 = i\nu(\mathscr{E}_0 t_0)\exp(-\nu^2/2)$. Equation (2.10) then yields

$$\frac{E_{on}(\tau,\zeta)}{\mathscr{E}_0} = \exp(-\tau^2/2)\left(\zeta + \tau - \zeta^2\sqrt{\pi/2}\exp\left[\frac{(\tau-\zeta)^2}{2}\right] \times \{s(\zeta) + \mathrm{erf}[(\tau-\zeta)/\sqrt{2}]\}\right). \quad (4.4)$$

For both of these signals the solution is centroantisymmetric, $E_{on}(\tau,\zeta) = -E_{on}(-\tau,-\zeta)$.

As pulse (4.3) propagates, its total on-axis energy per unity area, Eq. (3.6), decreases as

$$w(\zeta) = 1 - 2\zeta^2 + 2\zeta^3\sqrt{\pi}\exp(\zeta^2)[s(\zeta) - \mathrm{erf}(\zeta)]. \quad (4.5)$$

Similarly as for Eq. (3.7), one can show that in the limit $\zeta \to \infty$ all the terms in Eq. (4.5) larger than $O(\zeta^{-2})$ cancel one another, and $w(\zeta) \approx (3/2)\zeta^{-2}$. The evolution of the profile and the spectrum of the on-axis single-cycle Gaussian pulse as it propagates away from the source is depicted in Fig. 2; one can clearly see the formation of a 3/2-cycle pulse.

5. MULTICYCLE (OSCILLATING) PULSES

As the number of oscillations within a pulse increases, the pulse's spectrum narrows and the pulse becomes a regular envelope signal. It would still be of interest to have an exact solution for higher-order pulses, i.e., 3/2-cycle, two-cycle, etc. pulses, to see how this transition from a subcycle to a multicycle (i.e., envelope) pulse is developed. One can develop the solution for a multicycle pulse by having high-order modes based on the functions in Eqs. (3.1) and (4.1a) or (3.4) and (4.3). This can be done, e.g., in the case of a Gaussian mode, by choice of the initial signal of the nth order in the form

$$[E_0(\tau)]_n = \mathscr{E}_0 \sum_{m=0}^{n} A_m \tau^m \exp(-\tau^2/2), \quad (5.1)$$

where the coefficients A_m are chosen in such a way as to secure the orthogonality of the set of modes, i.e., $\int_{-\infty}^{\infty}[E_0(\tau)]_n[E_0(\tau)]_k d\tau = 0$ if $n \neq k$. (One of the choices is a standard set of Hermitian polynomials.) Yet another approach is to use a natural choice of a Gaussian envelope modulated by an oscillating (i.e., sin or cos) function of time:

$$E_0(\tau) = \mathscr{E}_0 \cos(q\tau)\exp(-\tau^2/2) \quad (5.2a)$$

or

$$E_0(\tau) = \mathscr{E}_0 \sin(q\tau)\exp(-\tau^2/2), \quad (5.2b)$$

where $q = \omega_0 t_0$ is a dimensionless frequency of carrier oscillations and ω_0 is the original frequency of the carrier. In the limit $q \to 0$, Eq. (5.2a) becomes a half-cycle pulse [Eq. (3.4)], and Eq. (5.2b) becomes a single-cycle pulse [Eq. (4.3)] (to the factor q^{-1}). In the opposite limit, $q \gg 1$, Eq. (5.2) is a regular oscillating pulse with a Gaussian envelope. Signals (5.2a) and (5.2b) then are physically indistinguishable (except for a phase); for $q = O(1)$ the difference between them is that Eq. (5.2a) has a dc component and Eq. (5.2b) has not. In terms of the error function of a complex argument, a general solution [Eq. (2.10)] for the signal [Eq. (5.2a)] and $\zeta > 0$ is

$$\frac{E_{on}(\tau,\zeta)}{\mathscr{E}_0} = \exp\left(-\frac{\tau^2}{2}\right)\left[\cos(q\tau) - \zeta\sqrt{\pi/2}\exp\left[\frac{(\tau-\zeta)^2 - q^2}{2}\right](\cos[q(\tau-\zeta)] + \mathrm{Re}\{\exp[-iq(\tau-\zeta)] \times \mathrm{erf}(\tau - \zeta - iq)/\sqrt{2}\})\right], \quad (5.3a)$$

and for the signal [Eq. (5.2b)] and $\zeta > 0$ it is

$$\frac{E_{on}(\tau,\zeta)}{\mathscr{E}_0} = \exp\left(-\frac{\tau^2}{2}\right)\left[\sin(q\tau) - \zeta\sqrt{\pi/2} \times \exp\left[\frac{(\tau-\zeta)^2 - q^2}{2}\right](\sin[q(\tau-\zeta)] + \mathrm{Im}\{\exp[-iq(\tau-\zeta)] \times \mathrm{erf}(\tau - \zeta - iq)/\sqrt{2}\})\right]. \quad (5.3b)$$

The easiest pulse profiles to handle are the oscillating modifications of a signal [Eq. (3.1)]:

$$E_0(\tau)/\mathscr{E}_0 = \mathrm{osc}(q\tau)(1 + |\tau|)\exp(-|\tau|), \quad (5.4)$$

where osc is either a cos or a sin function, depending on whether, in the limit $q \to 0$, one wants to have a half-cycle or a single-cycle pulse, respectively. Similarly as for solutions (3.2) and (4.2), one can obtain solution (2.10) for these signals in terms of elementary functions. Of course, in the limit $q \gg 1$, all these solutions, including Eqs. (5.3), become a regular Gaussian solution for an envelope Gaussian beam; in particular, the on-axis intensity of the beam decreases as ζ increases, in the way expected from [Eq. (2.7)]:

$$w(\zeta) = |D(\omega_0, z)|^2 = [1 + (zc/\omega_0 r_0)^2]^{-1} = [1 + (\zeta/q)^2]^{-1}. \tag{5.5}$$

6. OFF-AXIS PULSE TRANSFORMATION

The lower-frequency radiation diffracts more strongly and hence is found mostly off axis, where, by the same token, the higher frequencies are weaker, both of which factors result in the lengthening of the pulse. The smaller the diffraction angle at the cut-off frequency, $\theta_d = ct_0/r_0 = r_0/z_d$ [$\ll 1$ because of (1.1)], the stronger this effect is. In the far-field area, $\zeta \gg 1$, we introduce the angle of observation, $\theta = r/z$, and an angular factor that is due to diffraction, $\Theta = \sqrt{1 + \theta^2/{\theta_d}^2}$, and approximate the spectrum [Eq. (2.6)] of the pulse as

$$S_{\text{off}}(\nu, \theta, \zeta) \approx i\nu\zeta^{-1} S_0(\nu) \exp[-(i\nu + \nu^2)(\theta^2/2{\theta_d}^2)]. \tag{6.1}$$

In the case of a half-cycle Gaussian initial temporal profile [Eq. (3.4)] this yields a single-cycle off-axis pulse in far-field area:

$$E_{\text{off}}(\tau, \theta, \zeta) \approx \left(\frac{\mathscr{E}_0}{\zeta\Theta^2}\right) \frac{\partial\{\exp[-(\tau - \tau_{\text{sp}})^2/2\Theta^2]\}}{\partial(\tau/\Theta)}, \tag{6.2}$$

where $\tau_{\text{sp}} = \zeta(\theta^2/2{\theta_d}^2)$ is a delay time that is due to the curvature of spherical wave front. The time-dependent term in relation (6.2) resembles relation (2.12); the main difference is that the off-axis pulse stretches in time by the factor Θ and its spectrum is squeezed by the same factor. The maximum amplitude of the field in relation (6.2) is inversely proportional to ζ, as expected; note, however, that this amplitude now has a Lorentzian spatial profile in the cross section, i.e., $(E_{\text{off}})_{\max} \propto \Theta^{-2} = [1 + (r/r_0\zeta)^2]^{-1}$, instead of the original Gaussian spatial profile [Eq. (2.4)]. Similarly, in the case of single-cycle Gaussian initial temporal profile [Eq. (4.3)], relation (6.1) yields a 3/2-cycle off-axis pulse in far-field area:

$$E_{\text{off}}(\tau, \theta, \zeta) \approx \left(\frac{\mathscr{E}_0}{\zeta\Theta^3}\right) \frac{\partial^2\{\exp[-(\tau - \tau_{\text{sp}})^2/2\Theta^2]\}}{\partial(\tau/\Theta)^2}, \tag{6.3}$$

which is also stretched in time by the same factor Θ as in relation (6.2). Note that the cross-sectional spatial profile here is Θ^{-3}, instead of Θ^{-2} as in relation (6.2). This result is due to the narrowing of the spectrum of a single-cycle pulse compared with that of a half-cycle pulse.

7. LOW-FREQUENCY-LIMIT PROPAGATION

In the so called low-frequency limit $r_0 \ll ct_0$, the opposite of Eq. (1.1), with the source size much smaller than the wavelength $\lambda = 2\pi c/\omega$ of any frequency component, all the components have the same dependence on the angle of propagation; also, the initial spatial profile of the field becomes unimportant. The radiation pattern at each frequency is then determined by a spherical wave of an elementary (i.e., pointlike) dipole formed by the field distribution, $\mathbf{E}_0(t, x, y)$. At a distance $\rho = (x^2 + y^2 + z^2)^{1/2} \gg r_0$ from this pointlike source (i.e., away from the small near-field area $\rho_{\text{near}} \ll \lambda$), and assuming that the field $\mathbf{E}_0$ is linearly polarized, the spectrum of radiative waves is

$$S(\omega, \rho, \theta) = \frac{i\omega \cos\theta}{2\pi\rho c} \int\int_{-\infty}^{\infty} S_0(\omega, x, y)\mathrm{d}x\mathrm{d}y, \tag{7.1}$$

where θ is now the angle between the z axis and the direction of propagation, $\mathbf{u}_k$ ($|\mathbf{u}_k| = 1$), in the plane of the vector of polarization, $\mathbf{e}_0 = \mathbf{E}_0/E_0$, and the observation point. The Fourier transform of Eq. (7.1) produces the same time-derivative profile everywhere:

$$\mathbf{E}(\tilde{t}, \rho, \theta) = (\mathbf{e}_E/2\pi\rho c)[\partial q_0(\tilde{t})/\partial\tilde{t}], \qquad q_0(t) = \int\int_{-\infty}^{\infty} E_0(t, x, y)\mathrm{d}x\mathrm{d}y, \tag{7.2}$$

where $\mathbf{e}_E = \mathbf{u}_k \times [\mathbf{e}_0 \times \mathbf{u}_k]$ is the polarization vector of radiative field, $|\mathbf{e}_E| = \cos\theta$. Equation (7.2) explains pulse transformation in simple terms of elementary dipole antennae driven by a current $i_0(\tilde{t}) = \partial q_0/\partial\tilde{t}$, which is induced by the dynamics of the dipole electrical charges at the dipole, q_0, that originate from the source field, E_0; hence the time-derivative temporal profile. Bearing in mind that for a Gaussian beam $q_0 = 2\pi {r_0}^2 \mathscr{E}_0$, Eq. (7.2) at $\theta = 0$ is consistent with the Gaussian on-axis far field [relation (2.12)], indicating that the results [expressions (2.8)–(4.5)] for the on-axis field are valid regardless of condition (1.1). Furthermore, in far-field area inequality (2.12) describes an on-axis field for any distribution, regardless of whether it is Gaussian.

The dispersion and the transformation of the pulse that are due to the propagation and diffraction can to great degree be reversed. The feasibility of that reversal is related to the time–space reciprocity manifested here by Eqs. (2.3) and (2.9) being invariant to the simultaneous sign reversal of time τ and distance ζ. This reciprocity results in the symmetry $E_{\text{on}}(\tau, \zeta) = E_{\text{on}}(-\tau, -\zeta)$ if $E_0(\tau)$ is a symmetric function as for a half-cycle pulse [see Eqs. (3.1)–(3.7)] and in the symmetry $E_{\text{on}}(\tau, \zeta) = -E_{\text{on}}(-\tau, -\zeta)$ if $E_0(\tau)$ is an antisymmetric function, as for a single-cycle pulse [see Eqs. (4.1)–(4.5)]. In practice, one can transform a diffracted pulse almost into its original temporal shape (except for its dc component) by reflecting its diffracted wave front, e.g., from a spherical concave mirror if the angular aperture of the mirror is significantly larger than the diffraction angle θ_d. This finding is even more valid for a pulse without an initial dc component, e.g., for a single-cycle pulse. If such a mirror has radius of curvature R_m and is situated sufficiently far from the source, with the distance between them being

$f_1 \gg z_d$, the pulse is focused again into a tight spot at distance f_2 determined by a standard optical mirror formula:

$$f_1^{-1} + f_2^{-1} = 2R_m^{-1}. \tag{7.3}$$

A focused pulse will have almost its original time shape, especially if it did not have a dc component. If $f_2 < f_1$, the area of this spot is smaller than that of an original spot, and the amplitude of the focused pulse is larger by the factor f_1/f_2. The residual distortion of the pulse (in particular, slight bipolarity of an initially unipolar HCP) will be due to lower-frequency diffraction losses at the mirror; the larger the mirror size, the smaller this effect. In the case of a pointlike source, pulse restoration can be achieved by use of a full ellipsoid of revolution with the source and observation points situated at the foci of the ellipsoid.

In conclusion, by analytically solving diffraction-induced transformation of pulses with arbitrary temporal profiles, including single-cycle and half-cycle pulses, we have found closed-form solutions for the propagation of most commonly used initial spatiotemporal profiles and explained the nature of time-derivative transformation in the far-field area for arbitrary pulses. Most of our analytical results are related to on-axis pulse shapes; we have shown, however, that the off-axis pulses in the far-field area are stretched in time and found how this effect depends on the angle of observation. Based on time–space reciprocity, the pulse transformation that is due to diffraction can be reversed, e.g., by reflection of a pulse from a spherical concave mirror. The results obtained here can be used for the temporal and Fourier spectroscopy of supershort near-cycle and subcycle pulses.

ACKNOWLEDGMENTS

The author thanks P. L. Shkolnikov for discussions. This research is supported by the U.S. Air Force Office of Scientific Research.

REFERENCES

1. M. Born and E. Wolf, *Principles of Optics*, 6th ed. (Pergamon, New York, 1980).
2. A. Siegman, *Lasers* (University Science, Mill Valley, Calif., 1986); A. Yariv, *Quantum Electronics* (Wiley, New York, 1989).
3. P. R. Smith, D. H. Auston, and M. S. Nuss, IEEE J. Quantum Electron. **24**, 255 (1988).
4. D. Grischkowsky, S. Keidin, M. van Exter, and Ch. Fattinger, J. Opt. Soc. Am. B **7**, 2006 (1990); R. A. Cheville and D. Grischkowsky, Opt. Lett. **20**, 1646 (1995).
5. J. H. Glownia, J. A. Misewich, and P. P. Sorokin, J. Chem. Phys. **92**, 3335 (1990).
6. B. B. Hu and M. S. Nuss, Opt. Lett. **20**, 1716 (1995).
7. R. R. Jones, D. You, and P. H. Bucksbaum, Phys. Rev. Lett. **70**, 1236 (1993); C. O. Reinhold, M. Melles, H. Shao, and J. Burgdorfer, J. Phys. B **26**, L659 (1993).
8. A. E. Kaplan, Phys. Rev. Lett. **73**, 1243 (1994); A. E. Kaplan and P. L. Shkolnikov, J. Opt. Soc. Am. B **13**, 412 (1996).
9. A. E. Kaplan and P. L. Shkolnikov, Phys. Rev. Lett. **75**, 2316 (1995); Int. J. Nonlin. Opt. Phys. Mater. **4**, 831 (1995); A. E. Kaplan, S. F. Straub, and P. L. Shkolnikov, Opt. Lett. **22**, 405 (1997); J. Opt. Soc. Am. B **14**, 3013 (1997).
10. M. van Exeter and D. R. Grischkowsky, IEEE Trans. Microwave Theory Tech. **38**, 1684 (1990); J. Bromage, S. Radic, G. P. Agrawal, C. R. Stroud, Jr., P. M. Fauchet, and R. Sobolevski, Opt. Lett. **22**, 627 (1997).
11. R. W. Ziolkowski and J. B. Judkins, J. Opt. Soc. Am. B **9**, 2021 (1992).
12. I. S. Gradshtein and I. M. Ryzhik, *Tables of Integrals, Series, and Products* (Academic, New York, 1980).